

Methane Quantification Performance of the Quantitative Optical Gas Imaging (QOGI) System Using Single-Blind Controlled Release Assessment

Chiemezie Ilonze¹, Jiayang (Lyra) Wang^{2,5*}, Arvind P. Ravikumar^{2,5}, Clay Bell^{3,4}, Daniel Zimmerle^{4,5*}

¹Department of Mechanical Engineering, Colorado State University, Fort Collins, CO 80523

²Department of Petroleum and Geosystems Engineering, The University of Texas at Austin, Austin, TX 78712

³BPX Energy, Denver, CO 80202

⁴Energy Institute, Colorado State University, Fort Collins, CO 80524

⁵Energy Emissions Data & Modeling Lab, The University of Texas at Austin, Austin, TX 78712

*Corresponding author: dan.zimmerle@colostate.edu

Abstract

Quantitative optical gas imaging (QOGI) system can provide rapid quantification of leaks detected by optical gas imaging (OGI) cameras across the oil and gas supply chain. A comprehensive evaluation of the QOGI system's quantification capability is needed for successful adoption of the technology. This study conducted single-blind experiments to examine the quantification performance of the FLIR QL320 QOGI system under near-field conditions at a pseudo-realistic, outdoor, controlled testing facility that mimics upstream and midstream natural gas operations. The study collected 357 individual measurements across 26 controlled releases with rates between 2 slpm to 88 slpm of compressed natural gas (CNG). The majority (75%) of measurements were within a quantification factor of 3 (quantification error of -67% to 200%) with individual errors between -90% and 831% (i.e. within a factor of 10). Quantification error decreased with increasing controlled release rates. Performance improved when viewing gas plumes against a clear sky as background and at calm wind speed conditions relative to other scenarios. Quantification error varied substantially when the same controlled releases were quantified from different camera positions.

Synopsis

Until recently, the OGI camera was limited to emissions detection. This study investigates the quantification accuracy of the FLIR QOGI tool; an add-on to the camera that quantifies detected emissions.

Keywords

Methane, QOGI, FLIR, emissions quantification, methane quantification, FLIR QL320

1. Introduction

Methane emissions mitigation is a critical element of the global transition to a low carbon future.^{1–3} As the major component of natural gas, methane’s global warming potential (GWP) is 84 – 87 times that of carbon dioxide over a 20-year time scale.⁴ Curbing methane emission is an effective strategy to reduce near term climate warming, thus allowing a longer time frame to reduce carbon dioxide emissions.⁵ The oil and natural gas (O&G) sector is the largest industrial source of methane emissions in the United States, contributing approximately 29% of total methane emissions in 2021.⁶ In November 2021, the Environmental Protection Agency (EPA) proposed updated rules for methane emissions reduction from the O&G industry.⁷ Additionally, starting in 2024, the Inflation Reduction Act (IRA) will impose a methane charge on emissions above certain threshold at O&G facilities.⁸ Thus, accurate quantification of methane emissions is important for effective policy implementation.

To reduce methane emissions, many jurisdictions implement regular leak detection and repair (LDAR) programs at O&G facilities.^{9–12} These LDAR surveys do not require emissions quantification. One regulatory-approved methodology for emissions detection during LDAR surveys is ground-based optical gas imaging (OGI).^{13,14} Ground-based LDAR surveys with an OGI video camera requires scanning equipment on site. While recent advances in emissions detection technologies use drones and aircraft for faster surveys with comparable detection limits, they typically provide equipment level attribution and cannot pinpoint emitting components. In addition, they often require days to process emissions data and notify operators of detected emissions.^{15–17} In contrast, personnel with handheld OGI cameras can detect, localize, and repair emitting sources as soon as they are identified.^{18,19}

Historically, OGI did not quantify detected leaks – emissions quantification was performed as an additional measurement step using other tools.²⁰ For example, in many recent studies that quantified emissions from component leaks, emission quantification was done using a hi-flow sampler (HFS) for sources detected by OGI.^{21–28} The HFS uses attachments to capture and direct emissions into the instrument to measure emission rates. Thus, successful measurement relies on safe access to the emitting sources. Sources that are unsafe, inaccessible, or too large for the attachments to cover cannot be quantified by HFS.

The quantitative optical gas imaging (QOGI) is an add-on system to an OGI camera (a tablet) that analyzes plume pixels from videos of hydrocarbon emissions captured by the OGI camera and quantifies emissions using proprietary algorithms.^{32–34} The QOGI system (OGI camera + QOGI tablet) is an approved method by the British Columbia Oil & Gas Commission (BCOGC) for comprehensive LDAR surveys.³⁵ Unlike the HFS method, the QOGI system does not require personnel to have physical contact with emission sources to complete measurements. Several manufacturers now offer QOGI systems including handheld and mounted solutions.^{36–38} The system tested in this study is the Teledyne FLIR™ QOGI system, which pairs a QL320™ quantification tablet with a handheld GF320™ OGI camera.

The quantification tablets were originally produced by Providence Photonics and are now offered directly by Teledyne FLIR. Several studies have examined the accuracy of the QOGI system.^{32,39,40}

In 2015, the Concawe air quality OGI ad-hoc group tested the quantification accuracy of the Providence Photonics QL100 QOGI tablet, a previous version of the FLIR QL320.⁴⁰ Three gases (propane, methane, and propylene) were released either individually or mixed together over 61 leak tests, 31 of which were quantified with emissions rates ranging from 10 g/hr to 998.7 g/hr and the associated quantification errors between -23% to 69%. Among the 4 quantified releases that contained methane (2 pure methane releases and 2 mix releases), the quantification error ranged from -12% to 0% with release rates between 49.7 g/hr and 169.7 g/hr. However, during the Concawe study, a cool towel was used as a backdrop which provided a more uniform background and enhanced the difference between the apparent temperature of the background and the gas plume temperature (ΔT). Five of the 31 measurements used the cool towel to enhance background of which quantification error ranged from -6% to -23%. Another assessment of the QL100 in 2015 by Abdel-Moati et al. showed an average quantification error of 24% with a standard deviation of 39% for methane-controlled release rates ranging from 54 g/hr to 109 g/hr. When tested on propane, the quantification error ranged from -17% to +43%. Finally, in 2019, the Alberta Methane Field Challenge (AMFC) project tested the Providence Photonics QL320 tablet (an older version of the FLIR QL320) by conducting approximately 50 controlled releases ranging from 565 g/hr to 36,000 g/hr. The study results showed an 18% underestimation bias with a linear regression coefficient of 0.82 [0.73, 0.92] over the tested emission rate range.^{39,41} Even though the quantification errors of individual estimates ranged from -90% to 330%, the quantification error when all measurements were aggregated was comparable to that of the HFS.²⁹ In summary, known existing literature on the QOGI system performance is based on previous versions of the equipment (hardware and software) and small sample sizes, and did not systematically investigate the factors that may impact quantification accuracy or repeatability in field conditions. While the QOGI system requires the operator to input various parameters such as wind speed, ambient temperature, distance to emitting source, and quantification background for quantification, existing literature has not systematically examined their impact on quantification accuracy and precision.

This study presents a systematic quantification performance assessment of the FLIR QL320 QOGI system under near-field conditions at the Methane Emissions Technology Evaluation Center (METEC), which can mimic release geometries, rates, and backgrounds encountered at typical O&G facilities. We evaluate the quantification accuracy of individual estimates, as well as the quantification precision when repeated measurements were conducted for different camera positions, emission source, and controlled release rate. We also investigate the impact of controlled release rates, distance to emitting source, measurement background, and wind speed on quantification accuracy. Finally, we use Monte-Carlo (MC) simulations to highlight the likely impact of quantification uncertainties associated with aggregated fugitive leak rates on regulatory methane mitigation policy implementation.

2. Methodology

2.1 Testing Facility

The study was conducted at METEC located at Colorado State University, Fort Collins, USA. The 8-acre outdoor facility simulates emissions typically associated with upstream and midstream operations. METEC consists of non-operational, surface O&G equipment like wellheads,

separators, flare stacks, and liquid tanks. About 200 emission sources are strategically located on the equipment such that a wide range of realistic fugitive and vent emissions scenarios can be actualized. Metered natural gas of known gas composition is transported through buried gas supply tubing from onsite compressed natural gas (CNG) cylinders to the emission points.

2.2 Experimental Design and Protocol

Measurements took place from June 20th to June 24th, 2022. The QOGI system tested consisted of a FLIR GF320 OGI camera and a FLIR QL320 QOGI tablet (henceforth “FLIR tablet”). The Providence Photonics QL320 QOGI tablet (henceforth “legacy tablet”), an older version of the FLIR tablet, was used as a backup whenever the FLIR tablet ran out of battery. Measurement data were collected by a field crew of 2 researchers who operated the equipment and collected the data. An additional researcher helped with data collection when available.

One of the field crew had previously attended the in-person QOGI training sessions provided by Providence Photonics. The field crew followed the user manual provided by FLIR when deploying the tablets.^{42,43} The tablets quantify emissions by analyzing the image of the plume captured by the OGI camera and operationalizing the tablets for quantification can be done either through “tethered” or “Q-mode” configuration. Under the “tethered” configuration, the camera and the tablet are deployed together in the field and connected using a USB cable such that live feed video from the camera is transferred to the QOGI tablet for quantification while the emission is under observation. Under the “Q-mode” configuration, the OGI camera records emission videos together with required input parameters (e.g. windspeed) and quantification is performed later by analyzing the videos on the QOGI tablet. In this study, emissions were quantified under the “tethered” configuration where possible, as this reflected the preferred deployment in field conditions. When the tethered configuration was unable to quantify emissions – typically due to interference in the imaging background – analysis was performed later using the “Q-mode” configuration.

This study evaluated only the quantification performance – i.e., it did not test the detection performance of OGI camera surveys, which is available in the peer-reviewed literature.^{19,44,45} The experiment was performed single-blind: the METEC facility operator had a list of components and controlled release rates to test which was unknown to the field crew performing the measurements. The testing process involved the following:

1. The METEC facility operator selected an emission source, initiated a controlled release, waited until the release rate was steady, then informed the field crew of the emissions location. The release rate was not communicated to the field crew. The METEC facility operator assigned each experiment a unique numeric identifier (ID) and communicated that to the field crew for documentation. An experiment was defined as a controlled release at a given rate flowing through a specified emission point. The rate of any controlled release was held constant across all measurements conducted within a single experiment. This represented a simplification of observed field conditions, where temporal variability of emissions has been observed in multiple studies.

2. The field crew identified an unobstructed view of the leak location and gas plume, considering wind direction and the location of the emitting equipment. As per operational requirements acquired during training, the field crew reviewed the plume image from the tablet to decide on the suitability of a camera position for measurement based on the plume image and background, and the platform of the camera tripod.
3. Once a favorable camera position was found, the field crew mounted the camera on a tripod and positioned it such that the emitting source was at the center of the measurement boundary shown on the tablet's screen. Parameter data required for quantification were inputted into the tablet which included wind speed (calm (0-1mph), normal (2-10mph), or high (>10mph)), distance to emitting source, leak type (point or diffuse), and ambient temperature. Ambient windspeed and temperature were measured using a handheld digital anemometer while distance was measured with a measurement tape. The overlay functions were enabled on the tablet to colorize the plume to increase visibility. The field crew also ensured that only the streaming image of the gas plume interacted with the measurement boundary and used the masking feature to remove other areas of visual disturbance (e.g. vegetation on the ground) when necessary. The field crew selected the viewing angle and distance from the emission source considering the minimum and maximum distance requirement as specified in the manual for the 23mm (24° FOV) camera lens – 5 and 54 feet from the emission source.⁴²
4. At each camera position, at least 3 consecutive individual measurements were taken on the tablet, starting when the tablet's 'capture' button turned green to indicate stable measurement conditions. "Stable" was defined in the manual as when the 10 second quantification result was within 10% of the 1-minute quantification result. For each measurement, the field crew documented the background of the plume measured (sky, equipment, or ground). In some instances, 3 successful measurements could not be completed from a selected location due to rapidly changing meteorological conditions.
5. For each experiment, the field crew attempted measurements from 3 different camera positions by repeating steps 2 - 4. Each camera position was assigned a unique ID as no two camera positions had the same measurement conditions. It took approximately 10 minutes to find new camera positions. Measurement duration varied substantially as in some cases highly variable meteorological conditions elongated measurement duration. Each new camera position resulted in a new distance to the emitting source and/or a different background/perspective of the gas plume. In some instances, fewer than 3 camera positions were identified for an experiment due to limitations in acceptable angle-of-view, environmental conditions, and/or meteorological conditions.
6. After completing all measurements for an experiment, the field crew notified the METEC facility operator to stop the controlled release to conclude the experiment. The next experiment was then conducted following the same steps with the next experiment performed either using same emission source operating at a different emission rate or an emission source in a different location.

2.3 Data Analysis

Individual measurements were identified by the camera position and experiment IDs. Release rates and gas composition data were obtained from METEC release logs at the end of the study. The study team applied response factors for gas species in the controlled release to correctly adjust estimates generated by the QOGI tool (SI section S.1). Measurement data were paired with the controlled release data using experiment ID. Quantification error was assessed for each pair described above following Equation 1. The 95% confidence interval (CI) on the mean errors were obtained as the 2.5 and 97.5 percentiles of the bootstrapped mean errors. Boxplots were primarily used to investigate the impact of the factors (i.e. windspeed, plume background, etc.) by categorizing elements of each factor into groups (e.g. windspeed – calm, normal, and high windspeeds) as Figure 2 below shows. Since during the measurements, the study team had limited control of the number of sample data points per group, we set a minimum threshold of 30 data points (based on the central limit theorem) as likely sufficient for statistically significant analysis. Additionally, the Mann-Whitney U and Kolmogorov-Smirnov tests were used to investigate if the error distribution of the groups for each factor investigated were statistically different at a significance level (p) of 0.05.

$$\text{Quantification Error} = \frac{\text{Measured Emission Rate} - \text{Controlled Release Rate}}{\text{Controlled Release Rate}} * 100\% \quad (1)$$

2.4 Study Limitations

- While METEC mimics real O&G upstream and midstream facilities, not all field conditions were replicated for this study. At METEC, no equipment is heated (which can improve or complicate ΔT) or pressurized (which can cool the plume due to Joule-Thompson cooling at the point of release), which is common for separators (liquid separation equipment) on production equipment. Also, the facility is not characterized by elevated background emissions concentration, equipment vibrations, and noise levels typical in real O&G facilities. All controlled releases were at a constant rate in this study; variable rates are often observed in field conditions, particularly for gas-powered pneumatic controllers. Additionally, all METEC controlled releases were at approximately atmospheric pressure at each emission point exit unlike in field conditions where gases are likely to escape at higher pressure hence improving ΔT due to the Joule-Thompson effect.
- OGI cameras are sensitive to hydrocarbons other than methane that have infrared absorption bands within the spectral range of the camera, particularly ethane and propane. The CNG utilized in this study had a mean gas composition by volume of 84.8% of methane, 8.5% of ethane, 0.7% of propane, and a trace amount of heavier hydrocarbons and other gases. In field conditions, gas composition varies. Upstream (production) emissions contain higher levels of ethane and propane than tested here, increasing camera response, while midstream and downstream emissions may lower levels of ethane and propane than tested here, lowering camera response.
- Field testing took place over a 5-day period during the summer of 2022 representing a limited range of tested weather conditions. Quantification performance during winter and other associated meteorological conditions were not evaluated.

- The QOGI system was evaluated on common components at O&G production facilities and may not represent performance in other O&G supply chain sectors.
- Controlled release rates in this study were designed to explore the range of emission rates seen on O&G facilities that would be candidates for QOGI quantification. However, these rates do not represent the distribution of emission rates at operating O&G facilities. To account for this difference, our analysis includes a Monte Carlo simulation that applies results from this study to observed component level measurements from a field study.
- Finally, prior work on OGI surveys indicated a strong correlation between the experience of the OGI operator and the probability of detecting emissions.¹⁹ Similar dependence may exist in quantification and should be evaluated when broader usage of QOGI would make it possible to statistically sample a range of experience levels in a controlled experiment.

3. Results and Discussion

3.1 Quantification Accuracy of Individual Measurements

In total, 357 measurements were conducted with the QOGI system across 73 camera positions and 26 experiments. Emissions from 4 additional experiments could not be quantified from any camera position due to poor imaging background (cloudy sky or weeds on the ground). Each experiment had a controlled release rate ranging from 2.2 to 88 standard liters per minute (slpm) (SI section S1.1 and S1.2), and 1 to 11 (mean of 4.9) successful measurements were conducted at each camera position. Each experiment included 1 to 6 camera positions (mean of 2.8) and 4 – 27 (mean of 13.7) total successful individual estimates per experiment. Eight types of components were used as emitting sources in this study: connector, control box, flange, pressure transducer, pressure release valve (PRV), temperature regulator, thief hatch, and valve packing. Since the legacy tablet was used as a substitute for the FLIR tablet, there was no direct performance comparison between the two. Measurements taken with the two tablets were combined for the analysis even though the FLIR QL320 tablet had a newer quantification algorithm than the legacy tablet. The two tablets showed similar trends when quantifying controlled release rates within the same range (SI section S2).

Figure 1 examines quantification accuracy of individual estimates. Figure 1(a) compares individual rate estimates against controlled release rates. A linear regression analysis with intercept set to zero indicates a regression coefficient of 1.27 (95% CI [1.13, 1.40]) – an overestimation bias of 27%. Since the mix of emitter sizes on real facilities differs from that in the study, these results should be used with caution. Across all estimates, individual relative errors ranged from -90% to +831% compared to -90% to +330% from the AMFC study even though the latter tested much larger rates.³⁹ Results show that 46% (N = 165) of individual estimates were within a quantification factor of 2 (-50% to +100%) of the controlled release rates while 75% (N = 266) individual estimates were within a factor of 3 (-67% to +200%).

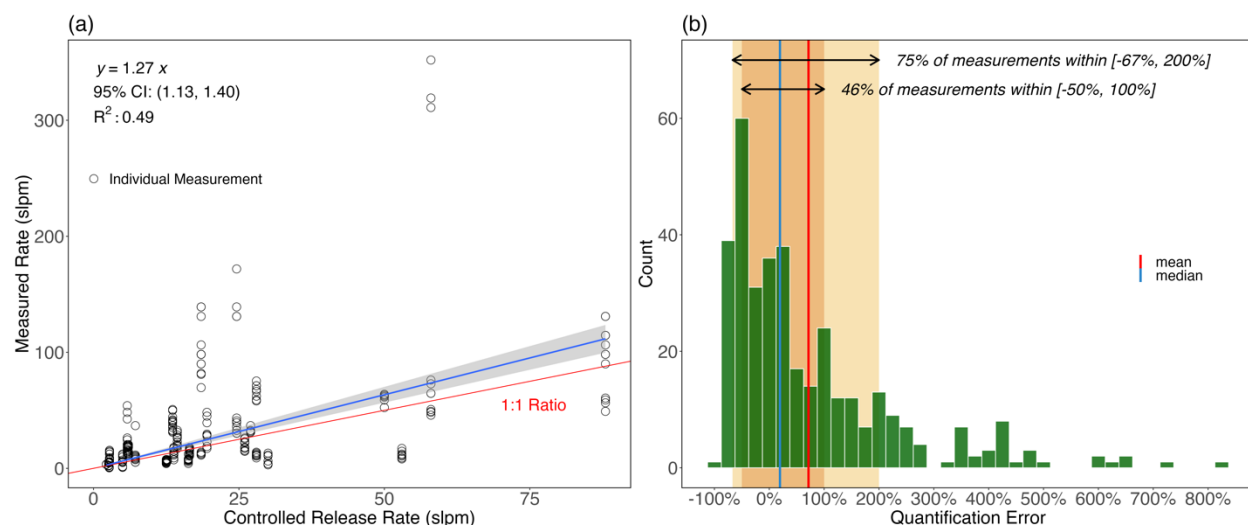
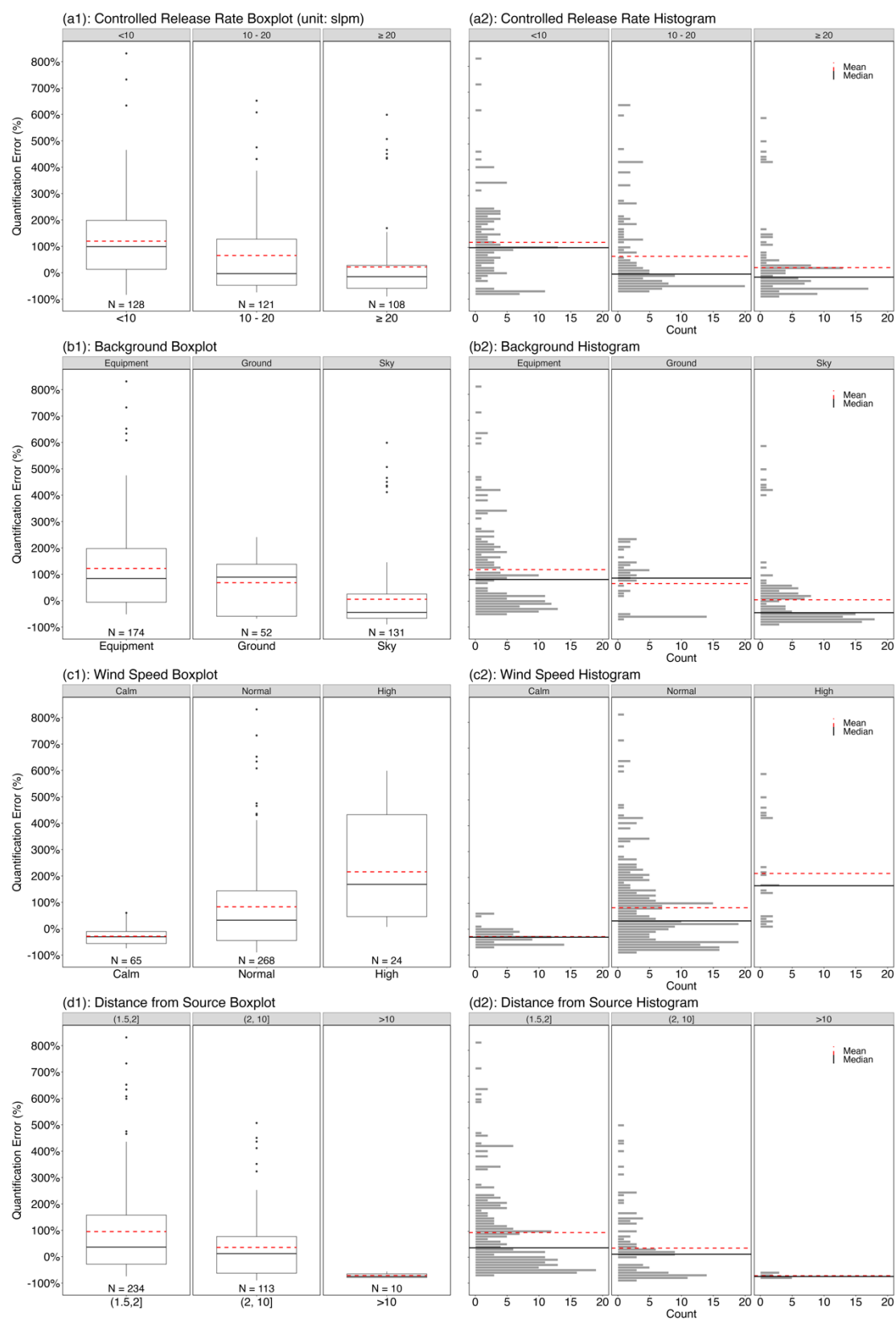


Figure 1: Quantification accuracy of individual estimates: (a) measured rates versus controlled release rate and (b) distribution of quantification error of individual estimates. In (a) the blue line represents linear regression through the origin with the gray shading showing the 95% confidence interval of the regression when bootstrapped. The red line represents the 1:1 ratio, where the measured rate matches the controlled release rate. In (b) the orange shading represents measured rate within factor of two of the controlled release rate (-50% to 100% quantification error), and the yellow shading represents measured rate within factor of three of the controlled release rate (-67% to 200% quantification error).

3.2 Impact of Quantification Parameters on Accuracy

3.2.1 Emission Rate

Figure 2 shows the impact of selected parameters on quantification accuracy, including (a) controlled release rate, (b) quantification background, (c) wind speed, and (d) distance from the emitting source. Mean (red dashed line) and median (black solid line) are shown in the box plots for each group. In Figure 2(a1), the controlled release rates tested were separated into three groups (see SI section S1.2): < 10 slpm, 10 – 20 slpm, and ≥ 20 slpm. The mean quantification errors for the groups were +119% (95% CI [+94%, +150%]), +65% (95% CI [+40%, +99%]), and +22% (95% CI [+0.3%, +53%]), respectively. The median quantification errors for the groups were 99%, -3%, and -15% respectively. Figure 2(a2) shows the distribution of quantification errors for each controlled release rate range. All 3 groups had positively skewed (mean > median) distributions that were significantly (statistically) different ($p < 0.05$) with mean errors inflated by outliers (see SI section S3.2). This type of positive skewness has been seen in several other studies of next-generation leak quantification methods.^{16,49} As controlled release rate increased, we observed improvement in quantification performance in three ways: 1) the mean error decreased, 2) the interquartile range decreased, indicating a narrower error distribution, and 3) the number and size of outliers decreased. One potential explanation for the observed improvement is that given that the QOGI system quantifies emissions by analyzing the pixel intensities of a gas plume image, larger emission rates lead to higher path integrated concentrations. This increases plume image contrast for the same ΔT and enhances the signal to noise ratio to improve quantification estimates.



312 Figure 2: Boxplots and distribution of quantification accuracy of individual estimates based on (a)
 313 controlled release rate, (b) quantification background, (c) wind speed, and (d) measuring distance

in meters. The black line in the middle of the box shows the median of the group and the dashed red line shows the mean of the group. The x-axis represents the groups within each parameter, and the y-axis shows the quantification error in percentage. The numbers at the bottom of the boxplots represent the sample sizes, which are numbers of individual estimates within each group.

The overestimation bias observed in this study was contrary to the conclusion of the AMFC study which showed 18% underestimation bias (regression coefficient of 0.82 (95% CI [0.73, 0.92])) by the QOGI system tested, but agrees with recent studies of other imaging systems that quantified emissions.^{39,49,50} The controlled release rate tested in the AMFC study ranged from 15 slpm to 925 slpm, which is about an order of magnitude higher than the rates in our study. A linear regression analysis of overlapping controlled release rates (15 slpm to 88 slpm) from both studies produced coefficients of 1.24 (95% CI [1.05, 1.44]) for our study (N = 169) and 1.14 (95% CI [0.72, 1.55]) for the AMFC study (N = 32). Although the AMFC study had smaller sample size and thus a wider confidence interval, the bias from both studies agrees. This result reinforces the observations from previous studies about the overestimation bias in the quantification of relatively small release rates which constitutes most of the fugitive emissions observed in traditional LDAR inspection. Additionally, results from the AMFC study showed the underestimation bias associated with the estimation of emission rates exceeding those tested in the current study. In general, our results suggest that users should exercise caution in using QOGI-based quantification estimates in developing emissions inventories or evaluating mitigation effectiveness.

3.2.2 Plume Background

During measurements, a gas plume background must provide a sufficient thermal contrast, commonly known as ΔT , for successful measurement. The QOGI tablets tested in this study requires a minimum ΔT of 2°C for quantification to be performed. Additionally, since the quantification method of the QOGI tablets track changes in the pixel intensity of infrared images, apparent temperature changes or disturbances in the background can interfere with identification of the plume boundary and/or affect quantification performance. These disturbances include but are not limited to shadows, glints, or reflections of heat sources on any metallic equipment, or by motion such as clouds or vegetation near the equipment. In this study, plume backgrounds were grouped into three categories: equipment, ground, and sky, as in Zimmerle et al.¹⁹ The field crew attempted to select camera positions during each experiment to include different backgrounds except in cases where this was not possible due to environmental limitations. A background was classified as “equipment” when the gas plume was viewed against either a different part of the same equipment (e.g., a well head casing) or against nearby equipment (e.g., a neighboring well head unit). A background was classified as “sky” when the plume was viewed against the sky, which may or may not have included cloud cover (e.g., an elevated emission source viewed against the sky). A background was classified as “ground” when the gas plume was viewed against the ground (i.e., sand, stones, gravels, vegetation). Results from various quantification backgrounds with statistically different error distributions ($p < 0.05$) are presented in Figure 2(b). The sample size of individual estimations with the ground as plume background was approximately a third of those quantified against equipment and sky backgrounds. Some parts of the ground at METEC were covered in vegetation that moved with the wind which made quantification challenging. The mean and median errors with ground as background were +68% (95% CI [+40%, +97%]) and 89%

respectively with more than half the sample size of each of other plume backgrounds. Estimates with equipment backgrounds had the highest mean and median errors of +122% (95% CI [+98%, +150%]) and 84% while measurements with sky backgrounds had the lowest mean and median quantification errors of +5% (95% CI [-13%, +32%]) and -44% respectively. While cloudy sky made quantification challenging, clear sky presented as the most favorable background for quantification compared to other backgrounds with the outliers as shown in Figure 2(b) driven by estimates at high windspeed (SI Table S4). This result supports findings from previous studies and recommendations on the FLIR's user manual where clear sky with low apparent temperature provided the best thermal contrast for the tablet's quantification algorithm.^{39,42,45}

3.2.3 Windspeed

Prevailing wind speed is a categorical parameter in the QOGI systems tested, with three defined levels: calm (0 – 1 mph), normal (2 – 10 mph), and high (>10 mph) under which 18%, 75%, and 7% of individual measurements were conducted respectively in this study. Results from the wind speed categories with distributions, which are statistically different ($p < 0.05$), are presented in Figure 2(c1) and Figure 2(c2). Result showed that the QOGI system was more accurate but likely to underestimate emissions in calm wind speed condition with a mean and median quantification error of -29% (95% CI [-35%, -21%]) and -31% respectively. Conversely, the wide interquartile error range along with a mean and median error of +216% (95% CI [+150%, +294%]) and 168% respectively indicates potential quantification challenges at high windspeed condition (note the small sample size: $N = 24$). This is likely due to turbulent and unsteady plume dispersion which can adversely affect the quality of plume detection. Measurements at normal wind condition with mean and median error of +83% (95% CI [+66%, +104%]) and 32% respectively, which is substantially higher and lower than that at calm and high windspeed conditions respectively, shows that quantification became challenging as windspeed increased.

3.2.4 Measurement Distance

For the QOGI tablets tested, acceptable measurement distance from the emitting source is a function of the camera lens.⁴² This study used a 23mm (24° FOV) OGI camera lens which limited measurement distance to between 1.5 m to 16 m (5 to 54 feet). To investigate the impact of measurement distance on quantification performance, measurement distances were grouped into three categories: 1.5 – 2 m, 2 – 10 m, and > 10 m. The FLIR and Legacy tablet's interface only allowed distance to be input in 0.5m increments hence all measured distances were rounded to the closest half-meter. Due to a very small sample size ($N = 10$), measurements at distances > 10 m are not considered in this discussion. As shown in Figure 2(d1), 66% of the measurements were performed within 2 m of the emitting source with a mean and median error of +95% (95% CI [+75%, +118%]) and +36% respectively. Similarly, 32% of the measurements were done within 2 – 10m of the emitting source with a mean and median error of +35% (95% CI [+14%, +62%]) and 12% respectively. With the error distributions of measurements from the distance categories 1.5 – 2 m and 2 – 10 m statistically different, and the estimates from the latter distance category having lower mean and median errors with tighter interquartile range around 0%, quantification performance likely improved with increasing measurement distance. This suggests that moving the camera closer to the emitting source did not necessarily result in better quantification performance. This result, however, should be taken with caution as additional data for

measurement distances > 10m will be needed for the trend of quantification accuracy with distance to be properly understood. As discussed earlier, the study team's decisions on measurement distance were primarily based on achieving clear and quality plume detection. While longer measurement distance may capture fuller plume dynamics on the camera thus improving quantification accuracy, it can also introduce visual noise from the background or adjacent components into the gas plume image which adversely affects quantification performance as observed in this study. Additionally, small, and low-pressure emissions tend to equilibrate quickly with the atmosphere as they exit the source, requiring the camera to be positioned closer to have a visible plume in the image. For example, more than half of measurements of rates <10 slpm were performed from distances between 1.5 – 2 m.

3.3 Observed Favorable Measurement Scenario

In actual field deployment, emission rate is always unknown until estimated. As discussed earlier, to estimate any emission, the measurement crew intentionally chooses the plume background and measurement distance, unlike the prevailing windspeed condition which is beyond human control. Table 1 summarizes the quantification performance of the QOGI tablets at different measurement scenarios (A - E) irrespective of the prevailing windspeed condition and release rate. While clear sky was earlier identified as the most favorable background for quantification, Table 1 shows that measurements from 1.5 – 2 m with plume background as equipment had the highest fraction of estimates within a factor of 2 (60%) with wide uncertainty, which reduced significantly ($p < 0.05$) to 24% (scenario B with a sample size < 30) when measurement distance increased to between 2 – 10 m. On the contrary, for measurements with sky as plume background, the fraction of estimate within a factor of 2 did not statistically change (was the same at approximately 49%) as measurement distances increased from 1.5 – 2 m to 2 – 10 m.

| Scenarios | Plume Background | Measurement Distance (m) | Sample Count | 95% Empirical C.I. of Error (%) | Percentage within a Factor of 2 [-50%, 100%] |
|-----------|------------------|--------------------------|--------------|---------------------------------|--|
| A | Equipment | (1.5, 2] | 149 | (-47, 639) | 60 |
| B | Equipment | (2, 10] | 25 | (7, 335) | 24 |
| C | Ground | (1.5, 2] | 52 | (-62, 241) | 21 |
| D | Sky | (1.5, 2] | 33 | (-68, 492) | 49 |
| E | Sky | (2, 10] | 88 | (-87, 432) | 49 |

Table 1: The Table summarizes quantification performance under different scenarios (plume background and measurement distance) in this study with sample count greater than 20. For each measurement scenario, quantification performance is illustrated with the 95% empirical confidence interval (C.I.) and the percentage of estimate within a quantification factor of 2 (-50%, 100%)

When prevailing windspeed condition was factored in as shown in Table S5 (in the SI), for scenario A, under calm windspeed (0-1 mph), the fraction of estimate within a factor of 2 increased to 100% with the associated uncertainty narrowing substantially. For scenarios D and E, under normal windspeed (2-10 mph), the fraction of estimates within a factor of 2 remained almost the same ($\pm 2\%$) although the sample size for scenario D was < 30. The impact of calm windspeed conditions

on scenarios D and E could not be analyzed due to insufficient data likewise normal windspeed condition for scenario A. In general, scenario A shows the coupling effect of other measurement conditions (some of which are favorable for accurate estimation) on quantification performance which illustrates that the users of the QOGI tablets tested in this study, in some cases, can obtain accurate estimates even when all favorable measurement conditions identified in this study does not co-exist. It is important to note that this study did not assess the quantification performance of QOGI for large emitters (> 10 kg/h) or super-emitters (> 100 kg/h), as defined by the US EPA in their proposed methane rule. Thus, the use of QOGI for emissions quantification and developing inventories should consider the large variance in performance observed in this study.

3.4 Quantification Precision

Quantification precision was evaluated by comparing the quantification error of individual measurements under the same camera position and the same experiment. As highlighted earlier, the field crew took 1 to 11 (average 4.9) successful measurements at each camera position and 4 – 27 (average 13.7) total successful measurements per experiment. Ideally, because the controlled release rates of each experiment remained approximately the same, the quantification errors of individual estimates under the same camera position were expected to be same, assuming the prevailing measurement conditions (e.g. wind speeds and background) remained consistent. Likewise, the quantification errors at various camera positions under the same experiment should be similar.

Figure 3 shows the quantification precision at (a) the camera position level and (b) the experiment level. In Figure 3(a), each marker represents one individual measurement – those stacked vertically with the same marker type were during the same experiment, and those with the same marker color are from the same camera position during that experiment. As controlled release rate increased, both the accuracy of measurements (mean error at a camera position) and precision of measurements (range of error observed at a camera position) improved, like findings from Figure 2(a). Note that the distribution of samples is not uniform across all emission rates. For example, 11% of measurements were conducted at controlled release rates ≥ 50 slpm. At the camera position level, the differences between the maximum and minimum error (henceforth precision range) spanned from 2% to 439% with 75% of camera positions having precision range <50%. All the 9 camera positions with precision range >100% had controlled release rates below 25 slpm; an emission rate range which also had high mean quantification error (Figure 2(a1)).

Figure 3(b) shows the quantification precision range at the experiment level. The whiskers represent the range of individual quantification errors obtained for each experiment, regardless of camera position. The markers represent the mean quantification error for each camera position. Each whisker connecting similar markers shows the range of quantification errors for an experiment. Shorter whiskers represent better precision. Results show that 11 camera positions (15%) were within $\pm 20\%$ of controlled release rates while 33 (45%) and 53 (73%) camera positions were within a factor of 2 (-50% to +100% error) and 3 (-67% to +200% error) of the controlled release rates, respectively. Of the 22 experiments that were quantified from 3 camera positions, the precision range was between 17% to 690% of the controlled release rate, indicating low measurement precision. Although the same release rate was measured throughout an experiment,

measurement conditions – measurement distance, plume background, windspeed, and wind direction – varied with camera position, substantially affecting quantification performance.

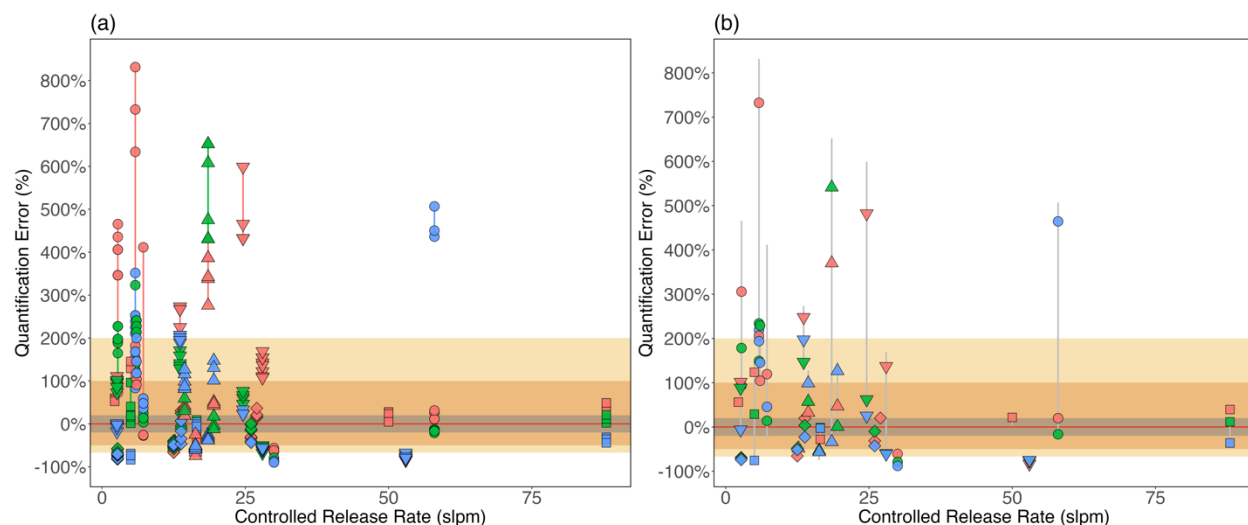


Figure 3: Quantification precision versus emission rate at (a) the camera position level and (b) the experiment level. The markers in (a) represent the error of individual estimates with whiskers representing the range of errors observed at each camera position. The markers in (b) represent the mean error from each camera position with whiskers representing the range of individual estimate errors during each experiment. For each group of vertically aligned markers, the colors represent estimates from the same camera position and the shapes represent estimates from the same experiment. The color and shape schemes are consistent between (a) and (b). The gray shading represents estimates within 20% of the controlled release rate (-20% to +20% quantification error). The orange shading represents estimates within a factor of two of the controlled release rates (-50% to +100% quantification error), and the yellow shading represents estimates within a factor of three of the controlled release rates (-67% to +200% quantification error).

3.5 Quantification Accuracy Simulation in Active O&G Facilities

While earlier results have shown the wide uncertainty on single estimates which can significantly impact emissions mitigation programs, some applications only prioritize quantification accuracy and the associated uncertainty when source-level estimates are aggregated at the facility or asset level. When all individual estimates and controlled releases in this study were aggregated, the QOGI system overestimated the total controlled release rate by 43% (95% CI [+23%, +55%]). To evaluate the potential quantification performance of the QOGI system during field deployments, we performed an MC analysis simulating facility-level quantification with its associated uncertainty. The analysis used the error distribution from this study and the component-level measurement data from Zimmerle et al.⁵¹ Measurement data from 150 facilities with rates within the tested range in this study (2slpm and 90 slpm) were considered as the true rates in the MC simulation with the number of leaks per facility ranging from 1 to 58 (mean of 6). Results from the MC simulations are shown in Figure 4 below.

Figure 4(a) shows the MC simulation (see SI section S5) analysis of the facility-level quantification error (with its associated uncertainty) for each of the 150 facilities from the field study.⁵¹ Results indicated that while on the mean, the aggregated estimates were within a quantification factor of 2 (-50% to 100%), the upper bound of the associated uncertainties (empirical 95% CI on the mean) was within a quantification factor of ~7. Unsurprisingly, the uncertainties became narrower as the count of measured emissions per facility increased which is consistent with the AMFC study and that of the Concawe air quality OGI ad-hoc group which identified similar trend for Method 21 correlations over large number of leaks.⁴⁰ To highlight the likely impact of quantification uncertainties on regulatory methane reduction programs like the IRA, the study performed an MC simulation assessing the mean error and the associated uncertainty for all 150 facilities aggregated. Figure 4(b) shows a cumulative distribution function (CDF) of the errors from the MC simulation with a mean error of +22.1% (empirical 95% CI of +13.2% to +31.4%). Assuming the simulated emissions from all the 150 facilities aggregated were above the threshold set by IRA and an operator owned all of them, the methane fee payment could vary from [\$1.8/hr to \$4.2/hr] at \$900/ CH₄ mt to [\$3.0/hr to \$7.1/hr] at \$1500/ CH₄ mt which could have substantial financial implications on operators.⁸

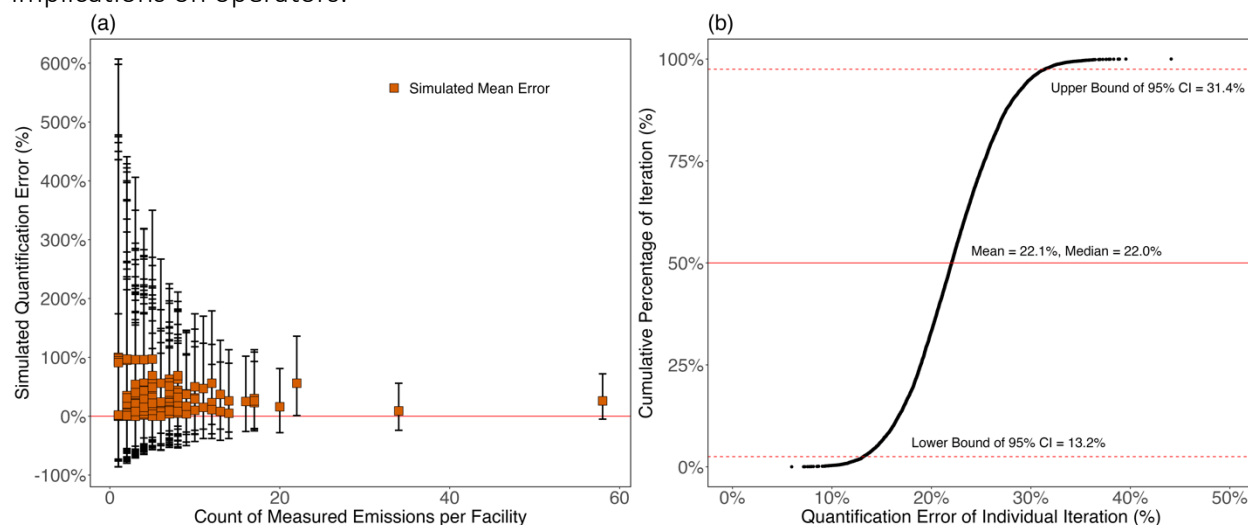


Figure 4: Monte-Carlo simulated quantification error by (a) count of measured emissions per facility and (b) total emissions from 150 facilities. In (a), the x-axis is the count of measured emissions on each facility and the y-axis is the simulated quantification error. The orange square represents the mean of quantification errors from the 10,000 Monte-Carlo simulations for each facility. The error bars represent 95% confidence intervals of the mean. In (b), the x-axis is rank ordered (CDF) quantification error of individual iteration, which represents quantification error of total simulated emissions from 150 facilities. The y-axis is the cumulative percentage of the count of iteration. The horizontal red solid line is the median of quantification error, and the horizontal red dashed lines are 95% confidence interval of quantification error.

4. Guidance

This study systematically investigates the impact of release rate, plume background, and selected user input data on the quantification performance of the FLIR QL320 QOGI tool. Results indicate wider quantification error range (-90% to +831%) than the prior study (-90% to +330%) that tested

similar QOGI tool, although the maximum rate in the current study was about an order of magnitude less than that of the prior study. Our result also shows a reduction in quantification error as release rate increased even though the tested rates were relatively low compared to prior studies. Further investigation will be needed to understand quantification performance for rates outside the tested range, especially larger rates (i.e. super emitters) which is an important emission source category.

Study results indicate combinations of conditions which are more favorable to quantification than other conditions, specifically calm windspeed (< 1 mph) and viewing emissions against a clear sky background. Since computational algorithms are proprietary, the cause of improved performance cannot be stated. However, less turbulent plume dispersion in calm winds provides imaging favorable for plume identification, as does viewing the emission plume against a clear sky where the sky's apparent temperature is usually low, improving thermal contrast needed for clear plume identification. Conversely, cloudy sky, vegetation on the ground, and/or backgrounds with poor ΔT were unfavorable for quantification. Although our results indicated that the distance range of 2m to 10m was more favorable for quantification, caution must be taken when applying this result as with available data, we could not reliably assess quantification performance for measurement distances > 10m.

The key control element for the study was the methodology applied by the OGI surveyors: The same method was used for all positions, all conditions. Controlling method removes operator experience and bias from the study design. Given that method was replicable across all experiments, the wide variation (up to 690%) in quantification performance as camera position changed highlighted that results are highly variable based upon camera position and potentially subtle changes in measurement conditions. Therefore, while an accurate estimate of emission is *possible* even when measurement conditions are not ideal, any estimate may differ significantly from the actual emission rate. In field practice, multiple estimates of one emitter is unlikely, and reported emissions will likely have error rates like aggregations of single estimates for each emitter on a facility.

The variation by camera position also implies that the experience level of the measurement crew at handling the OGI camera might substantially affect quantification accuracy. Hence, with the operationalization of the QOGI system in field deployment involving plume detection/visualization before quantification and results by Zimmerle et al.¹⁹ identifying surveyor's experience as the strongest predictor of detection rates, further studies would be needed to assess the impact of surveyor experience on quantification performance.

Author Contributions:

C. I. and J. W. contributed equally to this work. C. B. conceptualized and designed the research and organized the field measurement at METEC. A.P.R designed the research and provided the legacy tablet. C. I. and J. W. conducted the field measurement, data analysis and visualization, and wrote the manuscript. All authors participated in analysis discussion and manuscript revision.

Acknowledgements:

The authors would like to thank Rachel Day and Aidan Duggan from Colorado State University for assisting the field measurements and the FLIR team for lending us the FLIR QL320 tablet. The authors would also like to thank William Daniels from Colorado School of Mines for helping to interpret the statistical analysis. The authors acknowledge FLIR for the temporary access to a more recent QL320 tablet used in these experiments. FLIR personnel were not involved in the design or execution of the study or the subsequent analysis.

Competing Interests:

Subsequent to the field campaign, Clay Bell began working for bpx energy, headquartered in Denver, Colorado. bpx energy did not participate in the drafting of this paper and the views set forth in the paper do not necessarily reflect those of bpx energy.

Supporting Information:

The zip folder of the SI files contains additional details on study design, result analysis, and raw measurements data.

Reference:

- (1) US EPA, O. *Importance of Methane*. <https://www.epa.gov/gmi/importance-methane> (accessed 2023-04-04).
- (2) *The Future of Natural Gas: Markets and Geopolitics*; Colombo, S., El Harrak, M., Sartori, N., Istituto affari internazionali, OCP Policy Center, Eds.; Lenthe : European Energy Review: The Netherlands, 2016.
- (3) Gürsan, C.; de Gooyert, V. The Systemic Impact of a Transition Fuel: Does Natural Gas Help or Hinder the Energy Transition? *Renew. Sustain. Energy Rev.* **2021**, *138*, 110552. <https://doi.org/10.1016/j.rser.2020.110552>.
- (4) *Methane and climate change – Methane Tracker 2021 – Analysis*. IEA. <https://www.iea.org/reports/methane-tracker-2021/methane-and-climate-change> (accessed 2023-04-04).
- (5) US EPA, O. *Understanding Global Warming Potentials*. <https://www.epa.gov/ghgemissions/understanding-global-warming-potentials> (accessed 2023-02-07).
- (6) US EPA, O. *Overview of Greenhouse Gases*. <https://www.epa.gov/ghgemissions/overview-greenhouse-gases> (accessed 2023-05-22).
- (7) EPA's Supplemental Proposal to Reduce Pollution from the Oil and Natural Gas Industry to Fight the Climate Crisis and Protect Public Health: Overview.
- (8) Ramseur, J. Inflation Reduction Act Methane Emissions Charge: In Brief, 2022.
- (9) EPA. Leak Detection and Repair: A Best Practice Guide.
- (10) *Oil & gas compliance and recordkeeping | Department of Public Health & Environment*. <https://cdphe.colorado.gov/oil-and-gas-and-your-health/oil-gas-compliance-and-recordkeeping> (accessed 2023-03-16).
- (11) *40 CFR Part 98 Subpart W (up to Date as of 12-15-2022).Pdf*.

- (12) Branch, L. S. *Consolidated federal laws of Canada, Regulations Respecting Reduction in the Release of Methane and Certain Volatile Organic Compounds (Upstream Oil and Gas Sector)*. <https://laws-lois.justice.gc.ca/eng/regulations/SOR-2018-66/> (accessed 2023-05-10).
- (13) EPA. Appendix K - Determination of Volatile Organic Compound and Greenhouse Gas Leaks Using Optical Gas Imaging.
- (14) US EPA. *EPA Proposes New Source Performance Standards Updates, Emissions Guidelines to Reduce Methane and Other Harmful Pollution from the Oil and Natural Gas Industry*. <https://www.epa.gov/controlling-air-pollution-oil-and-natural-gas-industry/epa-proposes-new-source-performance> (accessed 2023-05-22).
- (15) Ravikumar, A. P.; Sreedhara, S.; Wang, J.; Englander, J.; Roda-Stuart, D.; Bell, C.; Zimmerle, D.; Lyon, D.; Mogstad, I.; Ratner, B.; Brandt, A. R. Single-Blind Inter-Comparison of Methane Detection Technologies – Results from the Stanford/EDF Mobile Monitoring Challenge. *Elem. Sci. Anthr.* **2019**, *7*, 37. <https://doi.org/10.1525/elementa.373>.
- (16) Bell, C.; Rutherford, J.; Brandt, A.; Sherwin, E.; Vaughn, T.; Zimmerle, D. Single-Blind Determination of Methane Detection Limits and Quantification Accuracy Using Aircraft-Based LiDAR. *Elem. Sci. Anthr.* **2022**, *10* (1), 00080. <https://doi.org/10.1525/elementa.2022.00080>.
- (17) Johnson, M. R.; Tyner, D. R.; Szekeres, A. J. Blinded Evaluation of Airborne Methane Source Detection Using Bridger Photonics LiDAR. *Remote Sens. Environ.* **2021**, *259*, 112418. <https://doi.org/10.1016/j.rse.2021.112418>.
- (18) Ravikumar, A. P.; Wang, J.; McGuire, M.; Bell, C. S.; Zimmerle, D.; Brandt, A. R. “Good versus Good Enough?” Empirical Tests of Methane Leak Detection Sensitivity of a Commercial Infrared Camera. *Environ. Sci. Technol.* **2018**, *52* (4), 2368–2374. <https://doi.org/10.1021/acs.est.7b04945>.
- (19) Zimmerle, D.; Vaughn, T.; Bell, C.; Bennett, K.; Deshmukh, P.; Thoma, E. Detection Limits of Optical Gas Imaging for Natural Gas Leak Detection in Realistic Controlled Conditions. *Environ. Sci. Technol.* **2020**, *54* (18), 11506–11514. <https://doi.org/10.1021/acs.est.0c01285>.
- (20) *Alternative Work Practice To Detect Leaks From Equipment*. Federal Register. <https://www.federalregister.gov/documents/2008/12/22/E8-30196/alternative-work-practice-to-detect-leaks-from-equipment> (accessed 2023-04-04).
- (21) Kuo, J.; Hicks, T. C.; Drake, B.; Chan, T. F. Estimation of Methane Emission from California Natural Gas Industry. *J. Air Waste Manag. Assoc.* **2015**, *65* (7), 844–855. <https://doi.org/10.1080/10962247.2015.1025924>.
- (22) Allen, D. T.; Pacsi, A. P.; Sullivan, D. W.; Zavala-Araiza, D.; Harrison, M.; Keen, K.; Fraser, M. P.; Daniel Hill, A.; Sawyer, R. F.; Seinfeld, J. H. Methane Emissions from Process Equipment at Natural Gas Production Sites in the United States: Pneumatic Controllers. *Environ. Sci. Technol.* **2015**, *49* (1), 633–640. <https://doi.org/10.1021/es5040156>.
- (23) Allen, D. T.; Torres, V. M.; Thomas, J.; Sullivan, D. W.; Harrison, M.; Hendler, A.; Herndon, S. C.; Kolb, C. E.; Fraser, M. P.; Hill, A. D.; Lamb, B. K.; Miskimins, J.; Sawyer, R. F.; Seinfeld, J. H. Measurements of Methane Emissions at Natural Gas Production Sites in the United States. *Proc. Natl. Acad. Sci. U. S. A.* **2013**, *110* (44), 17768–17773. <https://doi.org/10.1073/pnas.1304880110>.
- (24) Deighton, J. A.; Townsend-Small, A.; Sturmer, S. J.; Hoschouer, J.; Heldman, L. Measurements Show That Marginal Wells Are a Disproportionate Source of Methane Relative

- to Production. *J. Air Waste Manag. Assoc.* **2020**, *70* (10), 1030–1042. <https://doi.org/10.1080/10962247.2020.1808115>.
- (25) Li, H. Z.; Mundia-Howe, M.; Reeder, M. D.; Pekney, N. J. Gathering Pipeline Methane Emissions in Utica Shale Using an Unmanned Aerial Vehicle and Ground-Based Mobile Sampling. *Atmosphere* **2020**, *11* (7), 716. <https://doi.org/10.3390/atmos11070716>.
- (26) Ravikumar, A. P.; Roda-Stuart, D.; Liu, R.; Bradley, A.; Bergerson, J.; Nie, Y.; Zhang, S.; Bi, X.; Brandt, A. R. Repeated Leak Detection and Repair Surveys Reduce Methane Emissions over Scale of Years. *Environ. Res. Lett.* **2020**, *15* (3), 034029. <https://doi.org/10.1088/1748-9326/ab6ae1>.
- (27) Pekney, N. J.; Diehl, J. R.; Ruehl, D.; Sams, J.; Veloski, G.; Patel, A.; Schmidt, C.; Card, T. Measurement of Methane Emissions from Abandoned Oil and Gas Wells in Hillman State Park, Pennsylvania. *Carbon Manag.* **2018**, *9* (2), 165–175. <https://doi.org/10.1080/17583004.2018.1443642>.
- (28) Lamb, B. K.; Edburg, S. L.; Ferrara, T. W.; Howard, T.; Harrison, M. R.; Kolb, C. E.; Townsend-Small, A.; Dyck, W.; Possolo, A.; Whetstone, J. R. Direct Measurements Show Decreasing Methane Emissions from Natural Gas Local Distribution Systems in the United States. *Environ. Sci. Technol.* **2015**, *49* (8), 5161–5169. <https://doi.org/10.1021/es505116p>.
- (29) Connolly, J. I.; Robinson, R. A.; Gardiner, T. D. Assessment of the Bacharach Hi Flow® Sampler Characteristics and Potential Failure Modes When Measuring Methane Emissions. *Measurement* **2019**, *145*, 226–233. <https://doi.org/10.1016/j.measurement.2019.05.055>.
- (30) Alvarez, R. A.; Lyon, D. R.; Marchese, A. J.; Robinson, A. L.; Hamburg, S. P. Possible Malfunction in Widely Used Methane Sampler Deserves Attention but Poses Limited Implications for Supply Chain Emission Estimates. *Elem. Sci. Anthr.* **2016**, *4*, 000137. <https://doi.org/10.12952/journal.elementa.000137>.
- (31) Howard, T.; Ferrara, T. W.; Townsend-Small, A. Sensor Transition Failure in the High Flow Sampler: Implications for Methane Emission Inventories of Natural Gas Infrastructure. *J. Air Waste Manag. Assoc.* **2015**, *65* (7), 856–862. <https://doi.org/10.1080/10962247.2015.1025925>.
- (32) Abdel-Moati, H.; Morris, J.; Zeng, Y.; Corie II, M. W.; Ruan, Y.; Sanders, A. Hydrocarbon Detection & Quantification Using Autonomous Optical Gas Imaging Technologies. *J. Saf. Health Environ. Res.* **2017**, *13* (2).
- (33) Zeng, Y.; Morris, J.; Sanders, A.; Mutyala, S.; Zeng, C. Methods to Determine Response Factors for Infrared Gas Imagers Used as Quantitative Measurement Devices. *J. Air Waste Manag. Assoc.* **2017**, *67* (11), 1180–1191. <https://doi.org/10.1080/10962247.2016.1244130>.
- (34) Wilson, A. New Optical Gas-Imaging Technology for Quantifying Fugitive-Emission Rates. *J. Pet. Technol.* **2016**, *68* (08), 78–79. <https://doi.org/10.2118/0816-0078-JPT>.
- (35) British Columbia Oil & Gas Commission. Fugitive Emissions Management Guideline Version 1.0, 2019. <https://www.bc-er.ca/files/operations-documentation/Oil-and-Gas-Operations-Manual/Supporting-Documents/femp-guidance-july-release-v10-2019.pdf> (accessed 2023-05-22).
- (36) Abenza, C. *Gas leak quantification*. SENSIA. <https://sensia-solutions.com/gas-leak-quantification/> (accessed 2023-06-17).
- (37) *Gas Leak Detection Solutions - Opgal*. <https://www.opgal.com/quantitative-optical-gas-imaging-qogi/> (accessed 2023-06-17).

- (38) *Gas Cloud Imaging*. <https://pmt.honeywell.com/us/en/gas-cloud-imaging> (accessed 2023-06-17).
- (39) Singh, D.; Barlow, B.; Hugenholtz, C.; Funk, W.; Robinson, C.; Ravikumar, A. P. Field Performance of New Methane Detection Technologies: Results from the Alberta Methane Field Challenge. **2021**.
- (40) Concawe Air Quality Management Group. *An Evaluation of an Optical Gas Imaging System for the Quantification of Fugitive Hydrocarbon Emissions*; 2/17. https://www.concawe.eu/wp-content/uploads/2017/01/rpt_17-2.pdf.
- (41) Asgarpour, S. PTAC Methane Detection and Mitigation Initiatives Report.
- (42) FLIR. FLIR QL320 User Manual, 2020.
- (43) Providence Photonics QL320 User's Manual.
- (44) Zeng, Y.; Morris, J. Detection Limits of Optical Gas Imagers as a Function of Temperature Differential and Distance. *J. Air Waste Manag. Assoc.* **2019**, *69* (3), 351–361. <https://doi.org/10.1080/10962247.2018.1540366>.
- (45) Ravikumar, A. P.; Wang, J.; Brandt, A. R. Are Optical Gas Imaging Technologies Effective For Methane Leak Detection? *Environ. Sci. Technol.* **2017**, *51* (1), 718–724. <https://doi.org/10.1021/acs.est.6b03906>.
- (46) Wang, J. L.; Daniels, W. S.; Hammerling, D. M.; Harrison, M.; Burmaster, K.; George, F. C.; Ravikumar, A. P. Multiscale Methane Measurements at Oil and Gas Facilities Reveal Necessary Frameworks for Improved Emissions Accounting. *Environ. Sci. Technol.* **2022**, *56* (20), 14743–14752. <https://doi.org/10.1021/acs.est.2c06211>.
- (47) Vaughn, T. L.; Bell, C. S.; Pickering, C. K.; Schwietzke, S.; Heath, G. A.; Pétron, G.; Zimmerle, D. J.; Schnell, R. C.; Nummedal, D. Temporal Variability Largely Explains Top-down/Bottom-up Difference in Methane Emission Estimates from a Natural Gas Production Region. *Proc. Natl. Acad. Sci.* **2018**, *115* (46), 11712–11717. <https://doi.org/10.1073/pnas.1805687115>.
- (48) Johnson, D.; Heltzel, R. On the Long-Term Temporal Variations in Methane Emissions from an Unconventional Natural Gas Well Site. *ACS Omega* **2021**, *6* (22), 14200–14207. <https://doi.org/10.1021/acsomega.1c00874>.
- (49) Bell, C.; Ilonze, C.; Duggan, A.; Zimmerle, D. Performance of Continuous Emission Monitoring Solutions under Single-Blind Controlled Testing Protocol. ChemRxiv December 5, 2022. <https://doi.org/10.26434/chemrxiv-2022-4hc7q-v2>.
- (50) Bell, C. S.; Vaughn, T.; Zimmerle, D. Evaluation of next Generation Emission Measurement Technologies under Repeatable Test Protocols. *Elem. Sci. Anthr.* **2020**, *8*, 32. <https://doi.org/10.1525/elementa.426>.
- (51) Zimmerle, D.; Vaughn, T.; Luck, B.; Lauderdale, T.; Keen, K.; Harrison, M.; Marchese, A.; Williams, L.; Allen, D. Methane Emissions from Gathering Compressor Stations in the U.S. *Environ. Sci. Technol.* **2020**, *54* (12), 7552–7561. <https://doi.org/10.1021/acs.est.0c00516>.



747

748

For Table of Contents Only